Electronic structure of alkali-pnictide compounds

1992 J. Phys.: Condens. Matter 4 2449

(http://iopscience.iop.org/0953-8984/4/10/011)

J. Phys.: Condens. Matter 4 (1992) 2449–2474. Printed in the UK

Electronic structure of alkali–pnictide compounds

M Tegze†‡ and J Hafner‡

† Central Research Institute for Physics, Hungarian Academy of Sciences, H-1525 Budapest, *POB 49, Hungary*

‡ Institut für Theoretische Physik, Technische Universität Wien, A-1040 Wien, Austria

Received 25 November 1991

Abstract. We present an investigation of the electronic structure and the crystal binding in a number of metallic and semiconducting alkali–pnictide compounds based on self-consistent linear-muffin-tin-orbital (LMTO) calculations. We show that at all compositions the electronic structure is dominated by the strong attractive potential of the pnictide anions. In compounds with the 'octet' composition A_3B (A = alkali metal, B = Bi, Sb) we find a narrow gap separating the highest occupied anion band from the lowest empty cation band. The large difference in valence leades to a very large negative excess volume and a high electronic pressure on the alkali sites. This large electronic pressure leads to a lowering of the $(n-1)$d states relative to the ns states, especially for the heavy alkalis. As a consequence, the ionic gap in the octet compounds is very narrow and varies in a non-monotonic way in the series (Li, Na, K, Rb, Cs)$_3$–(Sb, Bi). At the equiatomic composition, the alkali–Sb compounds contain *infinite spiral Sb chains* stabilized by strong (ppσ) interactions. The bands close to the Fermi level are formed by bonding, non-bonding, and antibonding Sb p states, with the Fermi level falling into the gap between the non-bonding and the antibonding band. The Bi-rich alkali–Bi *compounds are metallic, but the electronic density of states still* bears the signature of the strong Bi potential.

1. Introduction

The intermetallic compounds of the alkali metals with elements of the fifth column of the Periodic Table (P, As, Sb, Bi) show a wide variety of chemical bonding properties. Naively, one expects a predominantly ionic bond. Because of the large eletronegativity difference the alkali metal transfers its single valence electron to the pnictide element, and the most stable compound is expected for the 'stoichiometric' composition A_3X (A stands for an alkali metal and X for a group-V element). The Bi compounds conform with this simple picture: a congruently melting A_3Bi compound with a $BiLi_3$ or $AsNa_3$ structure is the most stable phase in all alkali–Bi systems [1]. In accordance with a band-filling model for the metal–non-metal transition, the A_3Bi compounds are narrow-gap semiconductors. Besides the A_3Bi octet compounds, one finds congruently melting, close-packed metallic compounds (cubic Laves phases ABi_2 for the heavy alkali metals K, Rb, and Cs; and AuCu-type phases for the light alkali metals Li and Na). At equiatomic compositions, a deep eutectic minimum is found. Compounds of stoichiometry A_3Bi_2 and A_5Bi_4 have been reported for the heavy alkali metals, but their structures have not been resolved [3, 4]. The Sb compounds show a somewhat different phase diagram (figure 1). Again, a congruently

0953-8984/92/102449+26$04.50

melting octet compound with $AsNa_3$ or $BiLi_3$ structure exists in all alkali–Sb systems (except Cs_3Sb which is described as a disordered NaTl structure [5]); see table 1. In addition, all alkali metals except Li form monoantimonides ASb with NaP- and LiAs-type structures containing spiral Sb chains [6–8]. The monoantimonides are semiconducting. Based on structural arguments, a covalent bonding model with strong ($pp\sigma$) bonds along the chains has been proposed. The structures of the numerous compounds of intermediate stoichiometry are largely unknown. The octet compounds A_3Sb and the metallic compounds with stoichiometry A_3Sb_7 or ASb_2 (and close-packed structures) are congruently melting, with high melting points. The equiatomic compounds have a relatively low melting point; all A–Sb systems have a eutectic minimum close to the equiatomic composition. The variation of the depth of the eutectic suggests an increasing stability from NaSb to CsSb. The alkali–arsenic phase diagrams are similar to those of the Sb systems.

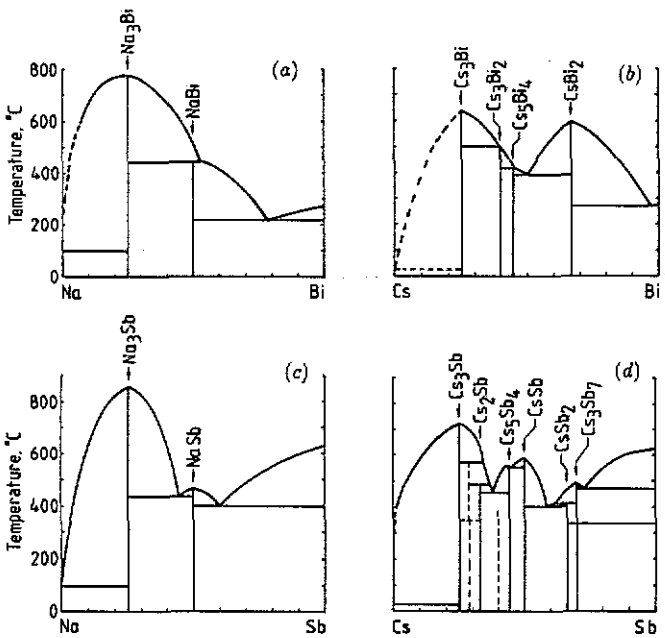

Figure 1. Phase diagrams of alkali–bismuth and alkali–antimony systems: (*a*) Na–Bi, (*b*) Cs–Bi, (*c*) Na–Sb, and (*d*) Cs–Sb. After [3].

The investigation of the liquid alloys creates additional interest in the physics of the alkali–pnictide alloys. As in many liquid alloys of the alkali metals with polyvalent elements [9], strong ordering effects and metal–non-metal transitions are observed. For the antimony compounds, it was shown that the semiconducting characteristics of the ASb and A_3Sb compounds are preserved on melting [10, 11], and this is also corroborated by a variety of thermodynamic [12] and structural investigations [13]: in liquid Na–Sb Redslob *et al* [11] found a steep conductivity minimum near the octet composition. In liquid K–Sb, a strong maximum of the Darken excess stability at the equiatomic compound was reported [12], and a second and even more significant peak is expected for the octet compound, where a well defined minimum in the electrical conductivity has been obtained [11]. For liquid Cs–Sb a broad resistivity maximum has been found around the equiatomic composition [10, 11]. From neutron

Table 1. Crystal structures of the alkali–pnictide compounds. **Boldface:** octet compounds:(1) BiF_3 structure; (2) $NaAs_3$ structure; (1, 2) $NaAs_3$-type at low temperature, BiF_3-type at high temperature; (3) disordered NaTl structure. *Italics:* polyanionic chain compounds: (4) NaP structure; (5) LiAs structure. Underlined: Close-packed metallic compounds: (6) $MgCu_2$-type Laves phase; (7) AuCu structure. (Compiled after Villars and Calvert [1]. Further references are given in the text.)

	Bi		Sb		As	
Cs	**Cs_3Bi**	(1)	**Cs_3Sb**	(3)		
			Cs_5Sb_2			
			Cs_2Sb			
	Cs_3Bi_2		Cs_3Sb_2			
	Cs_5Bi_4		Cs_5Sb_4			
			CsSb	(4)		
	$\underline{CsBi_2}$	(6)				
			Cs_3Sb_7			
Rb	**Rb_3Bi**	(1, 2)	**Rb_3Sb**	(2)	**Rb_3As**	(2)
			Rb_5Sb_2			
			Rb_5Sb_4			
			$RbSb_4$			
			RbSb	(4)	*RbAs*	(4)
	$\underline{RbBi_2}$	(6)	$RbSb_2$			
			Rb_3Sb_7		Rb_3As_7	
K	**K_3Bi**	(1, 2)	**K_3Sb**	(1, 2)	**K_3As**	(2)
	K_5Bi_4		K_5Sb_4			
			KSb	(5)	*KAs*	(4)
	$\underline{KBi_2}$	(6)	KSb_2			
Na	**Na_3Bi**	(2)	**Na_3Sb**	(2)	**Na_3Sb**	(2)
	$\underline{NaBi}$	(7)	*NaSb*	(5)	*NaAs*	(4)
Li	**Li_3Bi**	(1)	**Li_3Sb**	(1, 2)	**Li_3As**	(2)
			Li_2Sb			
	$\underline{LiBi}$	(7)			*LiAs*	(5)

diffraction investigations, Lamparter *et al* conjectured the existence of covalently bonded Sb chains in liquid Cs–Sb alloys [13, 14]. This is supported by the analysis of the magnetic susceptibility data which suggest that the liquid does not consist of fully ionized Cs^+ and Sb^{3-} ions [10]. Altogether, there seems to be evidence that the dominant type of ordering in in the liquid changes from salt-like charge ordering in Na_3Sb to covalently bonded polyanionic chains in CsSb. This would parallel the behaviour observed in the liquid alkali–Sn and alkali–Pb alloys, where the stoichiometry of the liquid 'compound' changes from the octet composition in Li–Pb and Na–Pb to that of the equiatomic compound in K–Pb, Rb–Pb, and Cs–Pb. In the alkali–lead systems, the equiatomic compounds contain P_4-like tetrahedral Pb_4^{4-} clusters. Like the formation of Te-like Sb^- chains in the A–Sb compounds, this is in accordance with the generalized Zintl principle [15, 16] for the formation of polyanionic cluster compounds. In any case, the liquid 'compound' corresponds to the most stable crystalline compound.

It is therefore rather surprising that the same behaviour is also observed in the alkali–Bi systems, although no equiatomic ABi compound exists. For the Li–Bi and Na–Bi systems, high resistivity maxima for the octet composition have been reported

[17, 18]; the excess stability of liquid Na–Bi shows a pronounced peak at the composition Na_3Bi [19]. For liquid K–Bi two peaks in the electrical resistivity have reported at 25 at.% and 40 at.% Bi [20], corresponding to two peaks in the excess stability at 25 at.% and 50 at.% Bi [21]. A similar behaviour of the thermodynamic properties has also been reported for liquid Rb–Bi [22]. For liquid Cs–Bi a single, extremely high-resistivity maximum has been observed [18] at 40 at.% Bi. Thus two problems arise: unlike in the alkali–Pb and alkali–Sb alloys, the maxima in the resistivity and in the excess stability indicating the existence of a cluster compound do not coincide, and there is no crystalline analogue to the liquid cluster compound CsBi. It is also rather enigmatic that the stability of the very stable crystalline octet compound Cs_3Bi is not reflected in the properties of the melt. Thus, in the alloys of the heavy alkali metals with Bi, a fundamental change in the chemical bonding properties must occur at melting.

The electronic properties of the crystalline compounds formed by the alkali metals and group-IV elements have been widely investigated [23–26] and it has been shown that the size ratio is the most important factor governing the competition between the two different mechanisms for compound formation. To date, only a rather preliminary study of the trends in the electronic structure of alkali–pnictide octet compounds has been presented [2]. A structure related to the NaTl-type Zintl lattice has been assumed for all A_3X compounds, and the band structure has been calculated using a non-self-consistent tight-binding technique. The tight-binding parameters were determined by scaling the transfer integrals fitted to a self-consistent pseudopotential calculation for LiAl (a NaTl-type Zintl compound) [27, 28]. It was concluded that all alkali–pnictide octet compounds should be considered as ionic, even though formal ionicities calculated in terms of local charges are small. However, in view of the approximations involved this conclusion cannot be considered very reliable. For the compounds $SbLi_3$ and $SbCs_3$ in the $BiLi_3$ structure, a self-consistent linear-muffin-tin-orbital (LMTO) calculation was reported by Christensen [29]. In agreement with the tight-binding calculations of Robertson [27, 28] which predict the Cs compounds to be more ionic than the Li compounds, Christensen concludes that the Li compound is rather covalent, with a strong Li–Sb bond. On the other hand, the Cs compound is considered as essentially ionic. Nonetheless, a systematic investigation of the octet compounds, especially of those with the hexagonal $AsNa_3$ structure, seems to be of interest. No investigation of the chain-like compounds has been published until now.

In this paper we present a comprehensive study of the electronic structure of alkali–Sb and alkali–Bi compounds, ranging from the octet compounds over the equiatomic compounds to the Laves phases. Our investigations are based on self-consistent LMTO calculations [30, 31]. We show that in all three types of compounds the electronic structure is entirely dominated by the deep anion potential, and that the valence states resemble closely the anion states. In the octet compounds they are very close to the wave functions of the free Bi (Sb) ions: the s states are strictly localized and only the p states interact to form a narrow band. The bonding is predominantly ionic, but in the compounds formed by the lighter alkali metals we find a distinct covalent contribution from bonds between the alkali atom and two of the three pnictide atoms.

The valence band of the equiatomic cluster compounds is very similar to the valence band of trigonal selenium and tellurium [32, 33]. The lowest band is a Bi (Sb) s band, which shows clearly the one-dimensional character of the Bi (Sb) chains. The Bi (Sb) p band is split into three parts: a bonding, a non-bonding, and an anti-

bonding (ppσ) band.The Fermi level falls into the gap between the non-bonding (or lone-pair) band and the antibonding band. This trimerization of the Bi (Sb) p band stresses the analogy of the bonding in the cluster compounds and in the chalcogenides. The strong covalent character of the Bi–Bi bands is evident even from the electronic structure of the ABi_2 Laves-phase compounds.

In the octet compounds, the lowest conduction band is an alkali band with a very strong d character and a varying degree of s–d hybridization. The strong d character of the lowest alkali states is a consequence of the strong volume contraction in the alkali–pnictide compounds, and is further enhanced in the Bi compounds by relativistic effects. In the cluster compounds the gap arises from the splitting of states that are bonding and antibonding within the chains. The antibonding Sb states overlap with the lowest alkali states, which have again a pronounced d character. Again the varying degree of overlap is related to the difference between the stabilities of the Sb and Bi cluster compounds.

Even the Bi-rich metallic compounds have a rather unusual electronic structure. The low-lying Bi s band is split into three parts, this splitting being characteristic for the dense tetrahedral network of the Bi atoms in the cubic AB_2 phases. The upper part of the valence band is formed by Bi p states only. The splitting between bonding and antibonding linear combinations of p states within the Bi tetrahedra subsists in the form of a deep pseudogap somewhat below the Fermi level. The alkali bands are again situated above the highest occupied Bi p state; they are strongly of d character.

Our paper is organized as follows. In section 2 we present very briefly the technical details of our calculations. Section 3 deals with the octet compounds, section 4 with the polyanionic cluster compounds, and sections 5 and 6 are devoted to the close-packed metallic compounds. Our conclusions are presented in section 7.

2. Technical details

We have used the LMTO method of Andersen *et al* [30, 31] in the atomic-sphere approximation (ASA). Scalar relativistic effects are included, but the spin–orbit interaction has been neglected. Exchange and correlation effects are described in a local-density approximation [34]; the potential is calculated self-consistently. The electronic density of states is computed using the linear tetrahedron method [35, 36]. The only inputs required are the positions and the atomic numbers of the constituent elements.

The radii of the atomic spheres taken as an approximation to the true Wigner–Seitz cells are calculated from the volumes of the compounds. All alkali–pnictide compounds have a large negative excess volume. It has been shown that the volume of formation of metallic and ionic s, p-bonded alloys and compounds is described to reasonable accuracy by low-order perturbation theory [37]. This simple calculation shows that the volume contraction affects mainly the more compressible alkali atoms. The apparent atomic volume of the alkali metals in the compound may be calculated by subtracting the atomic volume of the Bi (Sb) atoms in the pure element from the volume of the unit cell. For the compounds of the heavy alkali metals, this leads to a radius ratio close to unity. Details are given below, together with the crystallographic data.

The most significant approximations in our approach are the use of a spherically symmetric form of the potential, the ASA to the Wigner–Seitz cell, and the local-density approximation. It might be argued that the ASA is not well justified for

the cluster compounds, where the small number of Sb–Sb neighbours could lead to significant corrections to the muffin-tin potentials. In an LMTO–ASA treatment of the elemental semiconductors, one introduces 'empty spheres' such that a dense, close-packed arrangement of atomic spheres with minimal overlap is obtained. In the compounds, the role of the empty spheres is taken over by the alkali spheres. With the procedure for calculating the radius ratio introduced above, we get a dense packing of atomic spheres with minimal overlap. The comparison of the band structures of the chain-like compounds with the electronic structure of Se and Te obtained with pseudopotential techniques [32] suggests that the LMTO–ASA treatment is adequate, or at least an acceptable compromise between accuracy and efficiency. For these rather complicated structures computational efficiency is absolutely essential.

From extensive studies on small-gap semiconductors it is known that the effect of the local-density approximation is to underestimate the width of the gap. This should be kept in mind when we discuss the semiconductor properties of the octet and cluster compounds.

3. The octet compounds

The A_3Bi and A_3Sb compounds crystallize either in the $BiLi_3$ or in the Na_3As structure; some compounds show a temperature-induced polymorphic transition between a Na_3As-type low-temperature phase and a $BiLi_3$-type high-temperature phase. The crystallographic data for the octet compounds are compiled in tables 2 and 3. The $BiLi_3$ (or BiF_3) structure may be viewed as a face-centred cubic Bi lattice, with two tetrahedral and one octahedral hole per unit cell filled up by the Li (F) atoms. The results show very clearly that this view of the structure is more appropriate than that of an ordered superstructure of a body-centred cubic lattice. The $AsNa_3$ lattice can also be considered as a stacking of close-packed layers of As, with inserted layers of Na. The As atoms form triangular arrays in a hexagonal close-packed stacking, the Na(2) atoms lie approximately at the centres of the tetrahedral interstices in this array. The Na(1) atoms are coplanar with the As atoms (figure 2). Altogether each As atom is surrounded by 11 Na at distances between 2.94 Å and 3.305 Å. The dimensional analysis in a Pearson plot suggests that the dimensions of the lattice are mainly determined by the As–Na(2) distances [38].

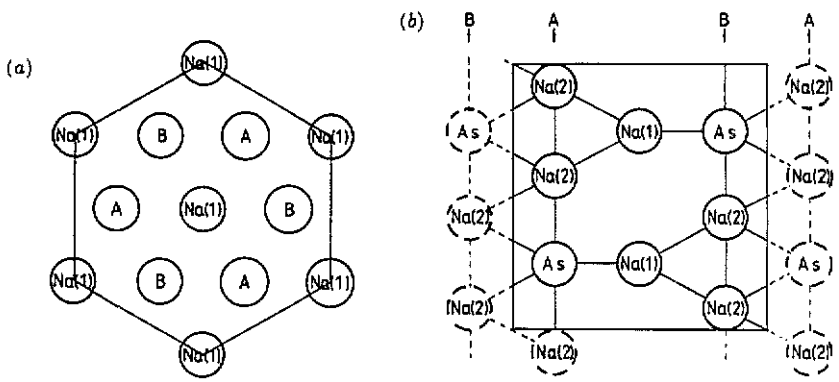

Figure 2. The Na_3As lattice. (*a*) View along the *c*-axis, (*b*) a section containing the *c*-axis. See text.

Table 2. Crystallographic description of the $BiLi_3$-type octet compounds.

Pearson symbol cF16, space group $Fm\bar{3}m$					
Atomic positions					
Bi	(4a)	0	0	0	
Li(1)	(4b)	0.5	0.5	0.5	
Li(2)	(8c)	0.25	0.25	0.25	
Coordination[a]					
	Bi	Li(1)	Li(2)	Li	Total
Bi	0	(6)	8	8 (+6)	8 (+6)
Li(1)	(6)	0	8	8	8 (+6)
Li(2)	4	4	(6)	4 (+6)	8 (+6)
Lattice constant, interatomic distances, Wigner–Seitz radius ratio, excess volume					
AB_3	a (Å)	d_{AB} (Å)	d_{BB} (Å)[b]	R_B/R_A	$\Delta\Omega$ (%)
$BiLi_3$	6.722	2.91	2.91 (3.03)	0.64	−24.0
$BiNa_3$[d]	7.933	3.43	3.43 (3.65)	1.00	−16.0
BiK_3 (HT)[c]	8.805	3.81	3.81 (4.52)	1.00	−31.6
$BiRb_3$ (HT)	8.898	3.85	3.85 (4.83)	1.16	−40.7
$BiCs_3$	9.310	4.03	4.03 (5.23)	1.16	−45.0
$SbNa_3$[d]	7.800	3.38	3.38 (3.65)	1.00	−17.2
SbK_3 (HT)	8.493	3.68	3.68 (4.52)	1.16	−37.3
$SbRb_3$ (HT)	8.840	3.83	3.83 (4.83)	1.20	−40.7
$SbCs_3$[e]	9.147	3.96	3.96 (5.23)	1.20	−47.1

[a] Values in parentheses indicate neighbours at distances that are only slightly larger than the distances of the direct neighbours.
[b] Values in parentheses give the interatomic distances in the body-centred cubic alkali metals.
[c] HT: high-temperature phase.
[d] *Hypothetical phases, see text.*
[e] Described as disordered Na–Tl-type in the literature.

The $BiLi_3$- and $AsNa_3$-type compounds differ appreciably in their excess volumes $\Delta\Omega$. They are distinctly larger in the $BiLi_3$-type phases. A simple first-order pseudopotential calculation leads to a reasonable estimate of $\Delta\Omega$. The analysis of the volume of formation of a large number of binary compounds has shown [37] that the first-order estimate is usually quite accurate for metallic and ionic compounds, whereas for covalently bonded compounds, the volume contraction is overestimated. The comparison of the $\Delta\Omega$ data for the octet compounds compiled in table 4 would suggest that the bonding is slightly more covalent in the $AsNa_3$ structure.

3.1. $BiLi_3$-type compounds

The total electronic densities of states of the A_3Bi (A = Li, Na, K, Rb, Cs) and of the A_3Sb (A = Na, K, Rb, Cs) compounds with the $BiLi_3$ structure are shown in figures 3 and 4. The partial densities of states and the band structures for $BiLi_3$, $BiRb_3$, $SbNa_3$, and $SbRb_3$ are given in figures 5 to 8. In general, the electronic structure conforms with the results expected for an octet compound: the lowest valence band is a very narrow Bi(Sb) s band; the highest occupied band is a Bi(Sb) p band. The alkali DOS contributing to both bands has a strongly mixed angular momentum character (figures

Table 3. Crystallographic description of the $AsNa_3$-type octet compounds.

Pearson symbol hP8, space group $P6_3/mmc$						
Atomic positions						
As	(2c)	0.333	0.667	0.25		
Na_1	(2b)	0	0	0.25		
Na_2	(4f)	0.333	0.667	0.583		
Coordination						
	As	Na_1	Na_2	Na	Total	
As	0	3	8	11	11	
Na_1	3	0	6	6	9	
Na_2	4	3	4	7	7	11
Lattice constants, interatomic distances, Wigner–Seitz radius ratio, excess volume						
AB_3	a (Å)	c (Å)	d_{AB} (Å)	d_{BB} (Å)[a]	R_B/R_A	$\Delta\Omega$ (%)
$BiNa_3$	5.453	9.674	3.154	3.233 (3.65)	1.00	−15.7
BiK_3 (LT)[b]	6.190	10.955	3.580	3.670 (4.52)	1.00	−26.9
$SbNa_3$	5.366	9.515	3.104	3.181 (3.66)	1.20	−17.3
SbK_3 (LT)	6.037	10.714	3.492	3.579 (4.52)	1.16	−30.8
$SbRb_3$ (LT)	6.283	11.180	3.634	3.725 (4.83)	1.20	−34.4
$SbCs_3$[c]	6.285	11.184	3.635	3.726 (5.24)	1.20	−47.1

[a] Values in parentheses give the interatomic distance in the body-centred cubic alkali metals.
[b] LT: low-temperature phase.
[c] Hypothetical phase, see text.

6 and 8). This suggests that at least for the compounds formed by the heavy alkalis, though perhaps not in those formed by the light alkali metals, the states contributing to the local DOS on the alkali sites are in reality pnictide states overlapping into the alkali atomic spheres. In the compounds formed by the lighter alkali metals, the alkali contribution to the lower peak of the upper valence band is mainly of s character, whereas the contribution to the upper peak has predominantly p character (figures 5 and 7). The DOS on the two inequivalent alkali sites are also different: the A(2) sites (which have four Bi (Sb) nearest neighbours) make a larger contribution to the valence band than the A(1) sites (which have only next-nearest Bi (Sb) neighbours). The lowest conduction band states are alkali states. Again we find a remarkable difference in the local DOS on the alkali sites: at the A(1) sites the lowest peak has a distinct s character, it is well separated from the rest of the conduction band. On the A(2) sites, the lowest peak has a stronger p character; an s peak appears at somewhat higher energy (figures 5 and 7). The larger contribution of the local A(2) DOS to the valence band together with the structure of the A(2) conduction band DOS suggests that there is some degree of covalent bonding between the Bi (Sb) p states and s, p-hybridized A(2) states. In the compounds formed by the heavy alkali metals, the strong volume contraction leads to a very high electronic pressure on the alkali sites. Combined with relativistic effects, this causes a lowering of the $(n-1)$d states relative to the ns and np states with the result that the lowest conduction band in (Rb, Cs)$_3$–(Sb, Bi) is a d band with some degree of (s,p)–d hybridization. A characteristic detail of the conduction band of the $BiLi_3$-type compounds is the very flat band tail at the lower edge of the band (which is hardly visible in the DOS plot, but see figures 5–8(a)

Table 4. Volume of formation of the alkali–pnictide compounds (in %).

Octet compounds	First-order calculation	Experiment ($BiLi_3$)	Experiment ($AsNa_3$)
$BiLi_3$	−25.2	−24.0	
$SbLi_3$	−29.0	−25.0	−15.5
$BiNa_3$	−37.3		−15.7
$SbNa_3$	−40.5		−17.3
BiK_3	−48.5	−31.6	−26.9
SbK_3	−50.9	−37.3	−30.8
$BiRb_3$	−51.5	−40.7	−29.0
$SbRb_3$	−53.6	−40.7	−34.4
$BiCs_3$	−54.4	−45.0	
$SbCs_3$	−56.4	−47.1	
Monoantimonides	**Calculation**	**Experiment**	
NaSb	−32.3	−12.3	
KSb	−46.2	−26.7	
RbSb	−50.3	−28.5	
CsSb	−54.7	−34.4	
Laves-phase compounds	**Calculation**	**Experiment**	
K_2Bi	−33.1	−23.7	
Rb_2Bi	−37.5	−28.9	
Cs_2Bi	−42.9	−35.3	

for the dispersion relations). This tail is absent only in the Li-based compounds. Owing to the small size of the Li ions, the electrostatic energy is large enough to push the Li s states sufficiently far above the Fermi energy that an indirect gap of 1.4 eV exists between the highest Bi p state at Γ and the lowest Li s state at the X point (figure 5). The Na octet compounds do not exist in the $BiLi_3$ structure, but we have calculated the band structure of hypothetical compounds Na_3Sb and Na_3Bi with the $BiLi_3$ lattice (the lattice parameters have been calculated on the assumption that the mean atomic volume is the same as in the $AsNa_3$-type phase). Because the lattice parameter is larger, the electrostatic energy is reduced, and the more extended Na s orbitals lead to a stronger Na–Na and Na–Sb interaction. As a consequence, the lowest Na s band has a large dispersion and crosses the Sb p-type valence band at the Γ point. The Na s band extends up to 2.45 eV above the Fermi level where a pseudogap marks the onset of the Na d states (figure 7). A similar structure is found in the compounds of the heavier alkali metals, with the difference, however, that the alkali s states are raised in energy relative to the alkali d states. In $SbCs_3$, the lowest Cs s state at Γ is only 0.2 eV lower than the lowest Cs d state (figure 8) and there is an indirect gap of 0.87 eV. A similar result holds for $BiCs_3$, with an indirect gap of 0.82 eV. Note that the gap in the Cs compounds is of a different nature to that in the Li compounds (see figures 5 and 8). It is important to realize that the shortest Cs–Cs distances in $BiCs_3$ and $SbCs_3$ are reduced by 23% (24%) relative to the interatomic distances in metallic Cs (see table 2). Under such high compression, Cs behaves as a

transition metal. The K- and Rb-based compounds show an intermediate behaviour: the tail of the alkali s band sticks out of the high density of states of the alkali d band and reduces the width of the indirect gap to about 0.57 eV in BiK_3 and $BiRb_3$ (see figure 6) and to about 0.40 eV in SbK_3 and $SbRb_3$. The gap is narrower in the Sb compounds because the smaller size of the Sb ion compared to the Bi ion leads to a larger overlap of the alkali orbitals.

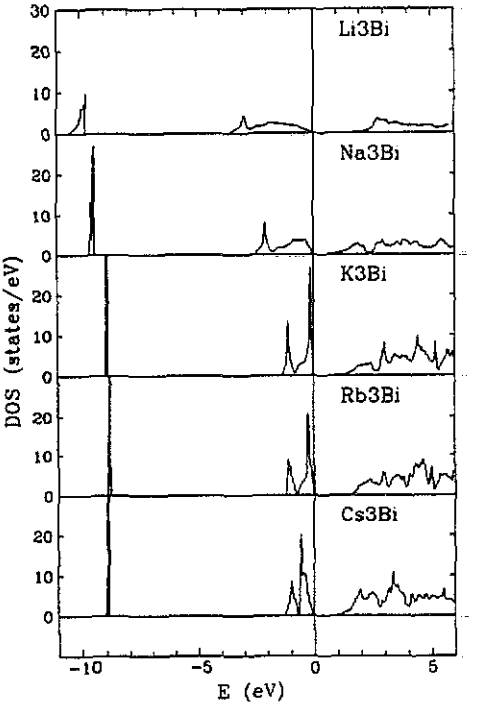

Figure 3. Total electronic density of states per eV and unit cell of the A_3Bi compounds (A = Li, Na, K, Rb, and Cs) in the $BiLi_3$ structure.

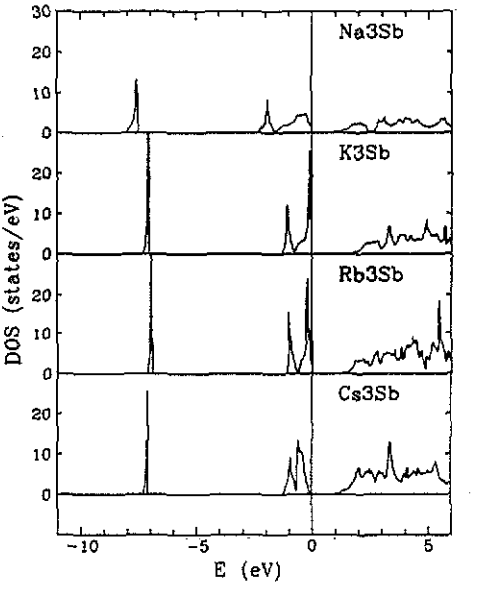

Figure 4. Total electronic density of states per eV and unit cell of the A_3Sb compounds (A = Na, K, Rb, and Cs) in the $BiLi_3$ structure.

Altogether, the trends in the octet compounds with the $BiLi_3$ structure are more complex than suggested by Robertson's non-self-consistent calculations [27, 28] with scaled tight-binding parameters. This study had predicted that the gap increases monotonically from the Li to the Cs compound. Our study shows that this is only partly correct. Except for $BiLi_3$, the largest gap is indeed found in the Cs compounds. In the Na compounds the extended Na s states interact strongly and form a broad band overlapping with the valence bands. In the compounds of the heavier alkali metals relativistic effects raise the s states relative to the d states and the lowest conduction band states acquire more d character. This leads to a re-opening of a narrow energy gap of a few tenths of eV. It will be rather hard to observe the true width of the gap in optical experiments because, e.g. in $BiRb_3$ (figure 6), the DOS of the s band is extremely small up to an energy of 1.0 eV above the bottom of the band. This energy marks the onset of the d band. Our results are in good agreement with the LMTO-ASA calculations of Christensen [29] for $SbCs_3$, concerning the nature and width of the gap. Christensen has also investigated the influence of spin–orbit

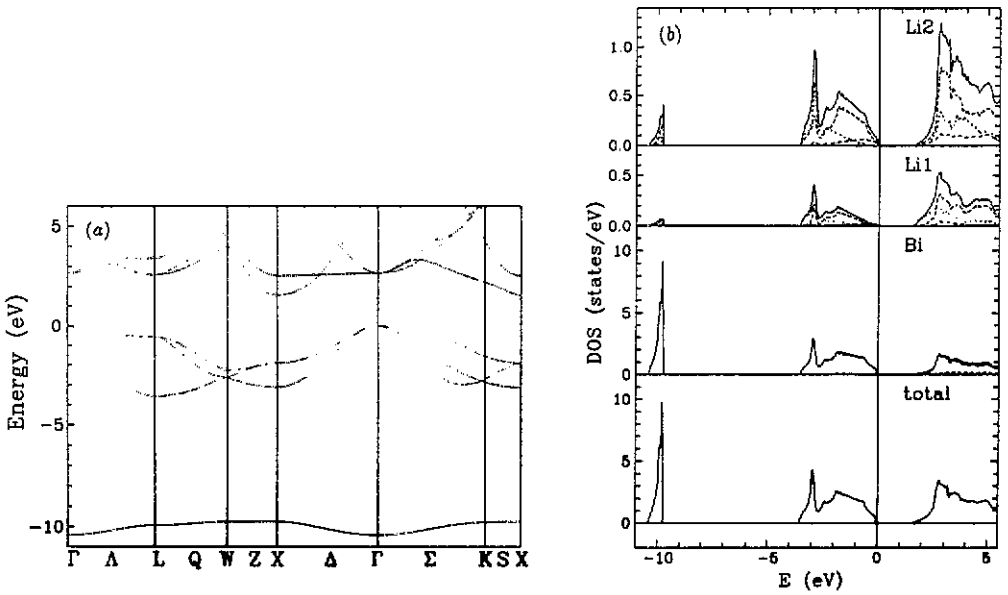

Figure 5. Band structure (*a*) and total, site- and angular-momentum-decomposed electronic density of states (*b*) per eV and unit cell for the compound $BiLi_3$. Full line—total DOS; dotted line—s states; dashed line—p states; dot-dashed line—d states.

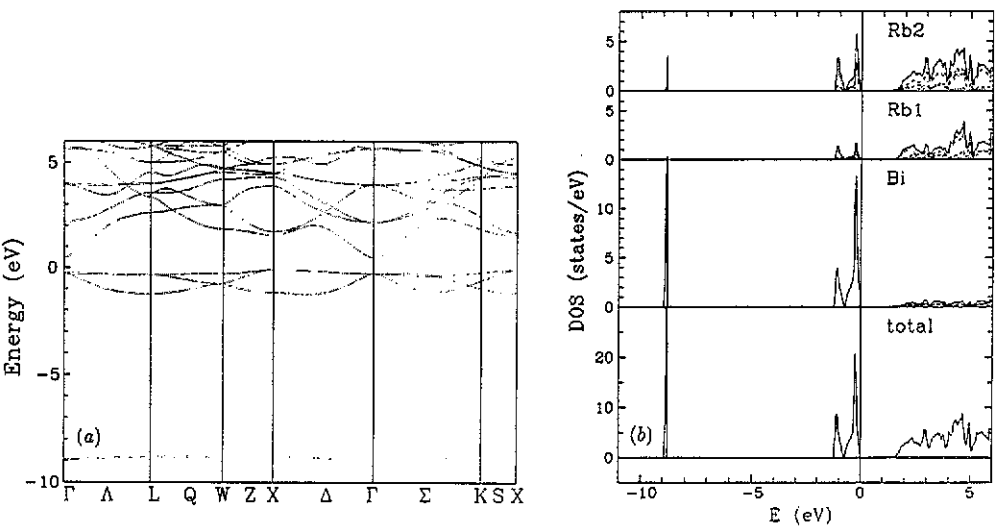

Figure 6. Band structure (*a*) and total, site- and angular-momentum-decomposed electronic density of states (*b*) per eV and unit cell for the compound $BiRb_3$ with the $BiLi_3$ structure. Key: see figure 5.

coupling and of a relaxation of the highest Cs core states. It is found that these effects have some quantitative influence on the results (width of the gap, predicted equilibrium lattice constant), but do not change the qualitative character of the band structure. Therefore, for an analysis of the trends, the scalar relativistic calculations

can be considered as sufficiently reliable. In agreement with Christensen's conclusions, our analysis of the local DOS suggests a certain degree of iono-covalent A(2)–Bi (Sb) bonding which is more pronounced in the compounds of the lighter alkali elements.

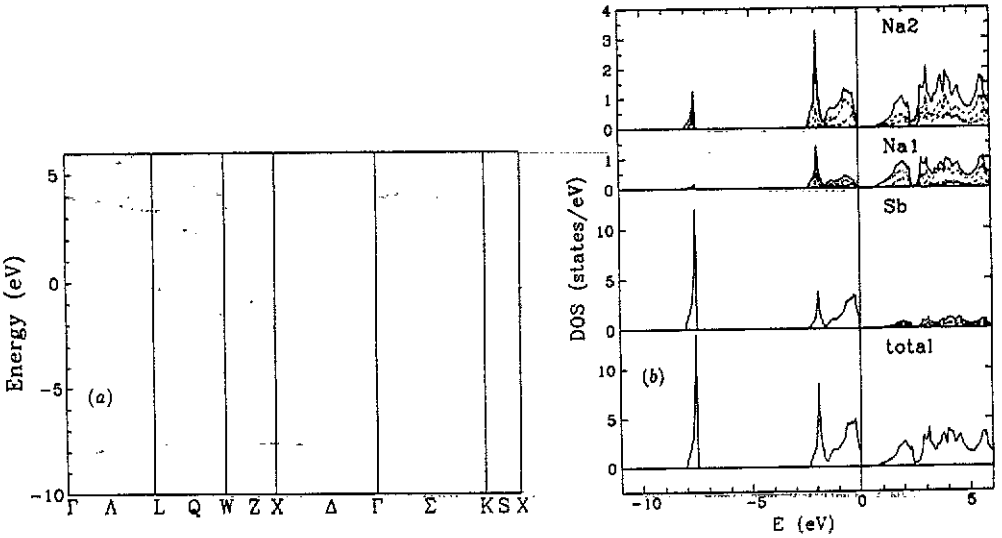

Figure 7. Band structure (*a*) and total, site- and angular-momentum-decomposed electronic density of states (*b*) for the compound $SbNa_3$ with the $BiLi_3$ structure. Key: see figure 5.

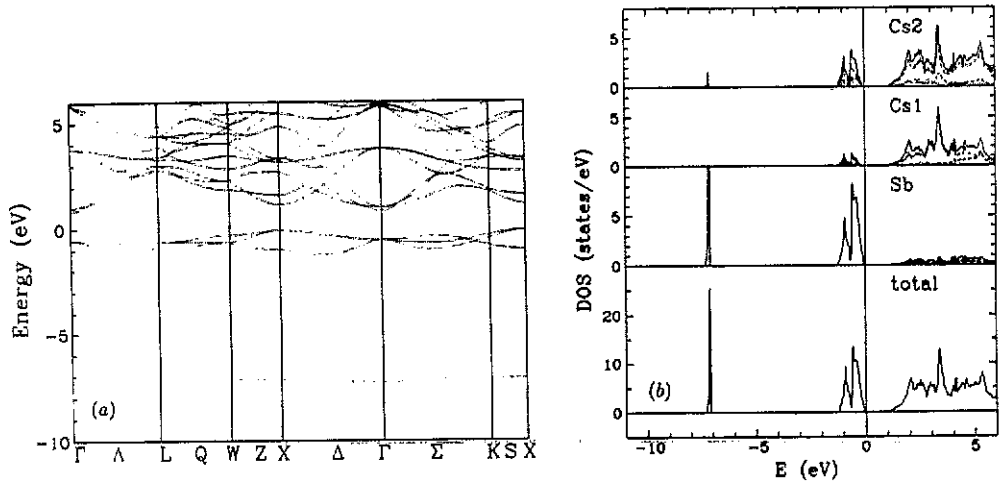

Figure 8. Band structure (*a*) and total, site- and angular-momentum-decomposed electronic density of states (*b*) for the compound Sb_3Cs with the $BiLi_3$ structure. Key: see figure 5.

3.2. $AsNa_3$-type compounds

In the $AsNa_3$ structure, there are eight atoms in the irreducible unit cell (compared with four in the $BiLi_3$ lattice), so the band structure and the electronic DOS are more

complex. In the $BiLi_3$ structure each atom has eight nearest neighbours plus six next-nearest neighbours at a distance that is only fifteen per cent larger (table 2). In the $AsNa_3$ structure each As and each Na(2) atom has eleven nearest neighbours, while each Na(1) atom has nine nearest neighbours. The reduced coordination numbers are not entirely compensated by an increased atomic volume, so in the $AsNa_3$ phases the alkali–pnictide distances are reduced by about five per cent, and the alkali–alkali distances by about three per cent compared with the values for the $BiLi_3$ phases. This is reflected in their electronic structure.

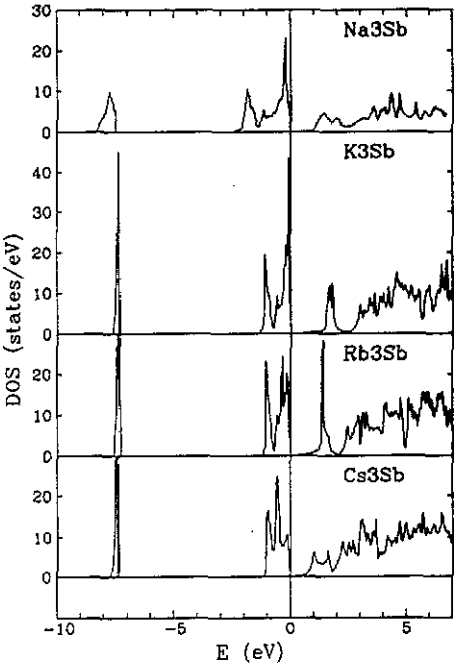

Figure 9. Total electronic density of states of the A_3Sb compounds (A = Na, K, Rb, Cs) in the $AsNa_3$ structure.

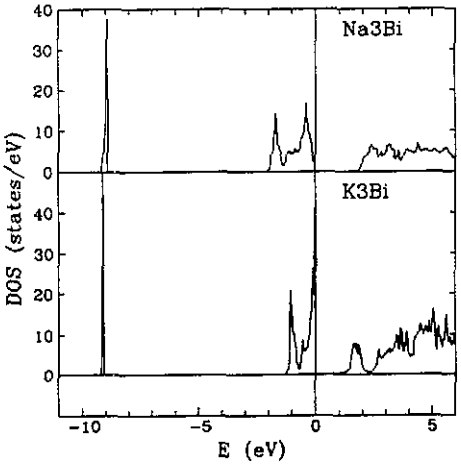

Figure 10. Total electronic density of states of the A_3Bi compounds (A = Na, K) in the $AsNa_3$ structure.

The total DOS of the antimony octet compounds with the $AsNa_3$ structure are given in figure 9, those for the bismuth octet compounds in figure 10. The overall form of the bands is the same in both structures: the valence bands consist of a low-lying pnictide s band and a pnictide p band close to the Fermi level. The s–p separation is somewhat larger than in the $BiLi_3$-type phases. In the Rb and Cs compounds we find again a strong s, p, d mixing in the valence band DOS on the alkali sites. In the Na and K compounds there is again a marked s–p splitting in the upper valence band (see also figures 11 and 13), suggesting a relatively strong (Na,K)–(Sb,Bi) bond.

This is also corroborated by the form of the conduction band. Compared with the $BiLi_3$-type phases, the shorter alkali–alkali distances lead to an even stronger reduction of the s character of the conduction band states at the alkali sites. A remarkable feature of the conduction electron states is the narrow band about 1.3 to 1.6 eV above the Fermi level. As the uppermost valence band, this band originates from

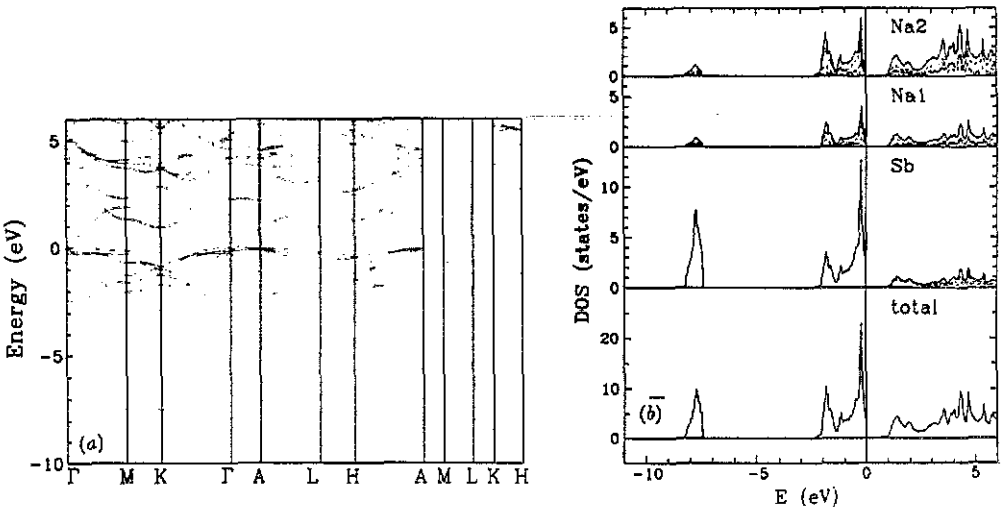

Figure 11. Band structure (*a*) and total, site- and angular-momentum-decomposed electronic density of states (*b*) for the compound $SbNa_3$ in the $AsNa_3$ structure. Key: see figure 5.

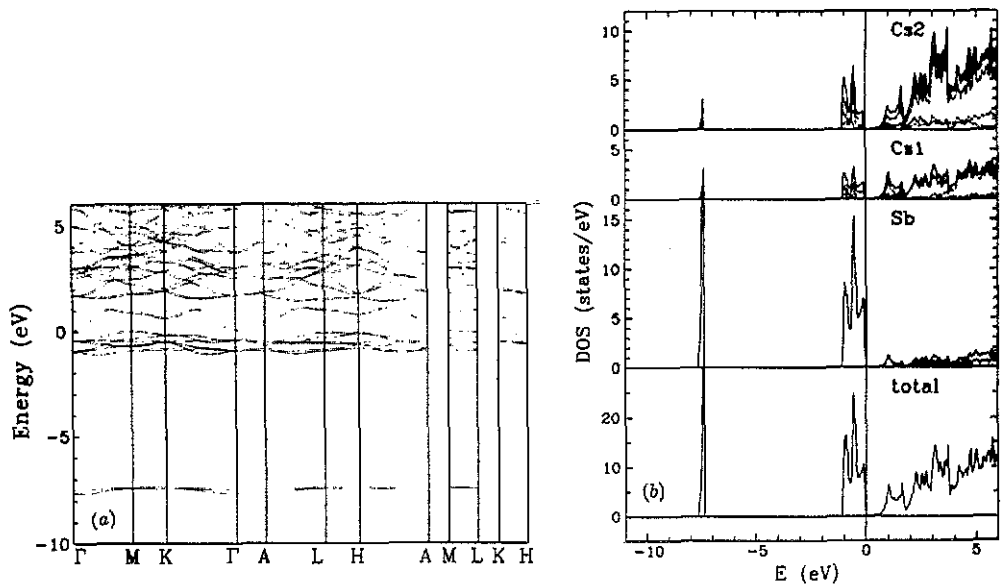

Figure 12. Band structure (*a*) and total, site- and angular-momentum-decomposed electronic density of states (*b*) for the compound $SbCs_3$ in the $AsNa_3$ structure. Key: see figure 5.

alkali–pnictide (ppσ) bonds; the Fermi level falls just into the bonding–antibonding gap (figure 11). The (ppσ) bonds are situated in the short Na(1)–As distances in the hexagonal plane and in the only slightly longer Na(2)–As distances along the hexagonal axis (see figure 2). Note that compared to the $BiLi_3$-type phases, the differences in the local DOS on the two inequivalent alkali sites is reduced. This relates to the

fact that in the $AsNa_3$ structure, all alkali atoms have direct pnictide neighbours (see table 3). Hence iono-covalent bonds can be formed on all alkali sites. This confirms our remarks on the at least partially covalent character of the $AsNa_3$-type phases. In the hypothetical compound $SbCs_3$, the Cs d character of the conduction band states is so strong that formation of a Cs–Sb ($pp\sigma$) bond is no longer possible (figure 12). Again the lowest conduction band has a low-energy tail, so all alkali–Sb octet compounds with the $AsNa_3$ structure are essentially zero-gap semiconductors.

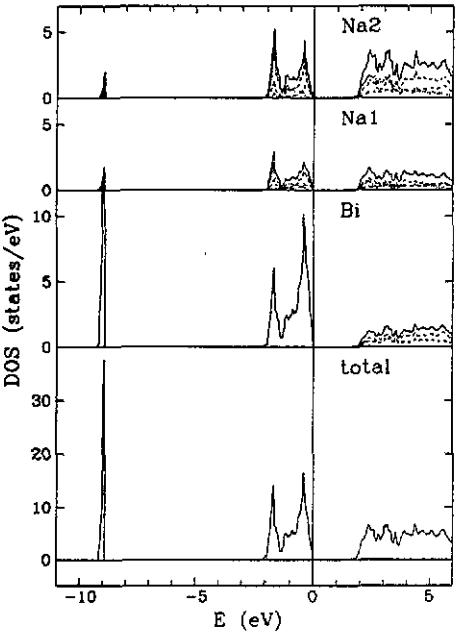

Figure 13. Total, site- and angular-momentum-decomposed electronic density of states for the compound $NaBi_3$ with the $AsNa_3$ structure.

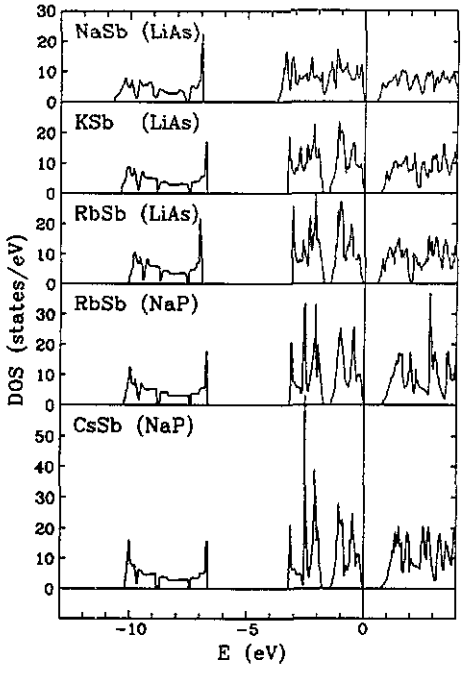

Figure 14. Total electronic density of states of the alkali monoantimonides: NaSb, KSb and RbSb in the LiAs structure and RbSb and CsSb in the NaP structure.

In the Bi compounds, the strength of the ($pp\sigma$) bonds is reduced due to the somewhat larger alkali–Bi distances (figure 13).

4. The monoantimonides

The equiatomic compounds of the lighter pnictide elements (P, As, Sb) with the alkali metals form complex structures with characteristic helical chains formed by the pnictide atoms. The crystallographic data for the monoantimonides of Na, K, Rb, and Cs are summarized in tables 5 and 6 (after [6–8]). NaSb and KSb crystallize in the monoclinic LiAs structure [6, 8]; RbSb and CsSb assume the orthorhombic NaP structure. Despite the difference in symmetry, the local coordination is very similar in both structures: the antimony atoms are arranged in infinite spiral chains, with bond angles varying between 106° and 114°. The alkali atoms may also be thought to

be arranged in spirals coaxial with the Sb helices, rotated by about 180° and with a larger spiral radius. The alkali–antimony coordination is rather irregular. On average each atom has six neighbours of the other kind arranged on a distorted octahedron. The intrachain distances between the antimony atoms are largely independent of the size of the alkali atom; they are close to the nearest-neighbour distances in elemental Sb. The bond angles and the torsion angles of the helices, however, increase with the size of the alkali atom. This suggests the following qualitative picture of the bonding in the monoantimonides: the alkali atoms transfer their single valence electron to the antimony atom. The Sb^- ion is isoelectronic with the Te atom, and the helical chains in the alkali monoantimonides are stabilized by Peierls-distorted ($pp\sigma$) bonds like those in trigonal Te. In Te, the Peierls distortion leads to a trimerization of the p band in a ($pp\sigma$) bonding, a non-bonding (or 'lone-pair') and a ($pp\sigma$) antibonding band. The ($pp\sigma$) bond determines the length of the intrachain bond, but the structure of the helix (bond and dihedral angles) are influenced by the lone-pair interactions. In the monoantimonides the alkali atoms isolate the Sb^- chains from each other and reduce the lone-pair interactions; hence the structure of the helices depends on their coordination. In trigonal Te, all bonds along the chain are equivalent. In the monoantimonides there are two crystallographically inequivalent bonds but the difference in the bond lengths is hardly larger than the standard deviations in the measurements. Along the chains, long and short bonds alternate. Alternating short and long bonds have also been found in isolated Te chains embedded in zeolite [39], and their bonding properties have been discussed by Fukutome [40].

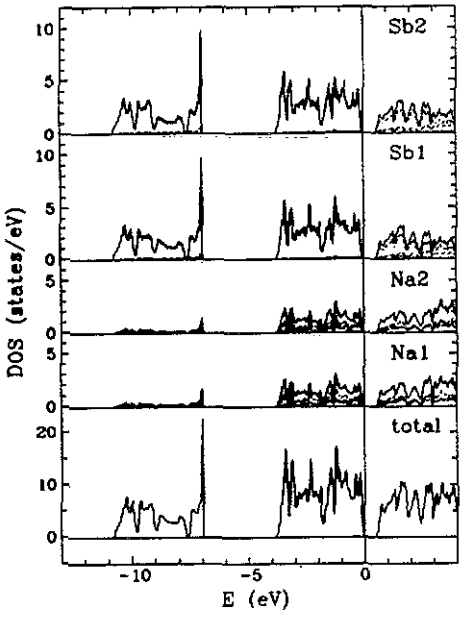

Figure 15. Site- and angular-momentum-decomposed electronic DOS in NaSb. Key: see figure 5.

The calculated electronic DOS of the monoantimonides (figure 14) confirms these conjectures. The lowest band is an Sb s band whose form is characteristic for a ($ss\sigma$)-bonded chain. The helical structure of the chain induces a characteristic splitting of

Table 5. Crystallographic description of the LiAs-type cluster compounds.

Pearson symbol mP16, space group $P2_1/c$

NaSb
a = 6.80 Å b = 6.34 Å c = 12.48 Å β = 117.6°

Na(1) (4e)	0.2108	0.3892	0.3251
Na(2) (4e)	0.2179	0.6725	0.0409
Sb(1) (4e)	0.3076	0.8994	0.2954
Sb(2) (4e)	0.2932	0.1599	0.1051

Coordination [a]

	Na(1)	Na(2)	Sb(1)	Sb(2)	Na	Sb	Total
Na(1)	0	2 (+1)	3	2 (+1)	2 (+1)	5 (+1)	7 (+2)
Na(2)	2 (+1)	1	3	3	3 (+1)	6	9 (+1)
Sb(1)	3	3	0	2	6	2	8
Sb(2)	2 (+1)	3	2	0	5 (+1)	2	7 (+1)

Interatomic distances (Å)
d_{Na-Na} = 3.43–3.85 d_{Na-Sb} = 3.12–3.42 d_{Sb-Sb} = 2.85, 2.86

Wigner–Seitz radius ratio R_{Na}/R_{Sb} = 1.2
Excess volume—12.3 %

KSb
a = 7.156 Å b = 6.917 Å c = 13.355 Å β = 115.7°

K(1) (4e)	0.2189	0.3990	0.3318
K(2) (4e)	0.2395	0.6668	0.0317
Sb(1) (4e)	0.3222	0.8991	0.2865
Sb(2) (4e)	0.3191	0.1662	0.1231

Interatomic distances (Å)
d_{K-K} = 3.86–3.98 d_{K-Sb} = 3.50–3.67 d_{Sb-Sb} = 2.83, 2.85

Wigner–Seitz radius ratio R_K/R_{Sb} = 1.36
Excess volume—26.7%

[a] Numbers in parentheses indicate neighbours at distances that are only slightly larger than the nearest neighbour distances given below.

the s band into four parts. The following bands are a bonding, a non-bonding, and an antibonding Sb p band. The Fermi level falls into the gap between the non-bonding and the antibonding band. In all four compounds, the antibonding band overlaps with the lowest alkali band. The partial DOS given in figures 15 and 16 confirm that the valence bands are indeed formed by pure Sb s and p states; the lowest alkali states are mainly of d character. The strong d character of the lowest alkali states is again the consequence of the strong contraction of the shortest distances between the alkali atoms, which are reduced by 6.6% (NaSb) to 22.7% (CsSb) compared with the interatomic distances in the pure metals. The total width of the occupied part of the valence band shows hardly any variation from NaSb to CsSb. This reflects the fact that the Sb–Sb distances are almost the same in all four compounds. The widths of the energy gap are E_g = 0.46 eV (NaSb), 0.68 eV (KSb), 0.50 eV (RbSb, LiAs-type), 0.68 eV (RbSb, NaP-type), and 0.65 eV (CsSb). The only significant change along

Table 6. Crystallographic description of the NaP-type cluster compounds.

Pearson symbol oP16, space group $P2_12_12_1$

RbSb
a = 7.315 Å b = 7.197 Å c = 12.815 Å

Rb(1) (4a)	0.4057	0.9244	0.0366
Rb(2) (4a)	0.1472	0.6574	0.3331
Sb(1) (4a)	0.3051	0.1603	0.2841
Sb(2) (4a)	0.4201	0.4240	0.1306

Coordination[a]

	Rb(1)	Rb(2)	Sb(1)	Sb(2)	Rb	Sb	total
Rb(1)	0	2	3	2 (+1)	2	5 (+1)	7 (+1)
Rb(2)	2	0	3 (+1)	3	2	6 (+1)	8 (+1)
Sb(1)	3	3 (+1)	0	2	6 (+1)	2	8 (+1)
Sb(2)	2 (+1)	3	2	0	5 (+1)	2	7 (+1)

Interactomic distances (Å)
d_{Rb-Rb} = 4.00, 4.03 d_{Rb-Sb} = 3.63–3.88 d_{Sb-Sb} = 2.85, 2,86

Wigner–Seitz radius ratio R_{Rb}/R_{Sb} = 1.40
Excess volume $\Delta\Omega = -28.05$

CsSb
a = 7.576 Å b = 7.345 Å c = 13.273 Å

Cs(1) (4a)	0.4138	0.9250	0.0316
Cs(2) (4a)	0.1430	0.6583	0.3348
Sb(1) (4a)	0.3151	0.1604	0.2804
Sb(2) (4a)	0.4242	0.4268	0.1358

Interatomic distances (Å)
d_{Cs-Cs} = 4.04, 4.16 d_{Cs-Sb} = 3.77–4.07 d_{Sb-Sb} = 2.84, 2.86

Wigner–Seitz radius ratio R_{Cs}/R_{Sb} = 1.40
Excess volume $\Delta\Omega = -34.4$ %

[a] Numbers in parentheses indicate neighbours at distances that are only slightly larger than the nearest-neighbour distances given below.

the series is a varying degree of overlap between the bonding and the non-bonding p bands—it is distinctly larger in NaSb than in the other three compounds. This relates to the variation of the ratio of interchain to intrachain Sb–Sb distances. This ratio is 1.45 in NaSb and varies between 1.63 and 1.65 from KSb to CsSb. The stronger interchain interaction broadens the p bands. The Na ions are just large enough to separate the Sb^- chains, so that the interchain coupling is weak compared with the intrachain coupling and the chain structure is stable. The unfavourable size ratio is also why there is no stable LiSb compound with the LiAs structure. There are also only small differences between the electronic DOS calculated for the two different structures. This is demonstrated in the example of a hypothetical RbSb with the LiAs lattice. The crystallographic data have been calculated on the assumption that the atomic volume in LiAs-type RbSb is the same as in the NaP-type phase, and that the reduced atomic coordinates are the same as in KSb (see table 5). The main

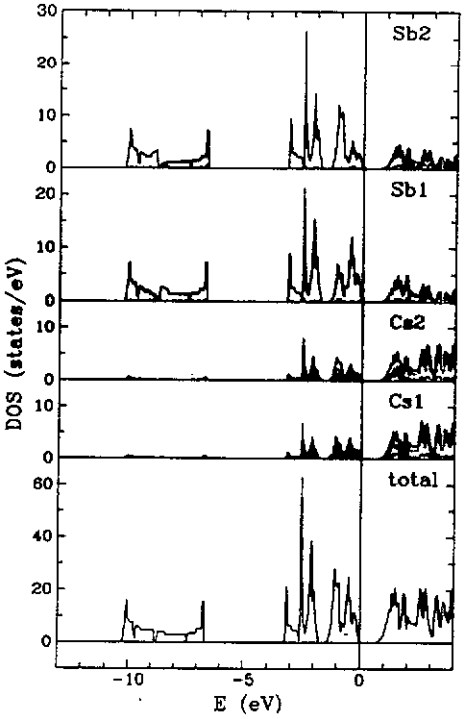

Figure 16. Site- and angular-momentum-decomposed electronic DOS in CsSb. Key: see figure 5.

difference betwween the two sets of data is in the overlap between the antibonding Sb p band and the lowest Rb band. Evidently this relates to the details of the Rb–Sb coordination.

Altogether, our results confirm the validity of a generalized Zintl principle [15, 16] for the formation of polyanionic cluster compounds: on alloying, the alkali atom transfers its single valence electron to the antimony atom, and the Sb^- ions form infinitely extended chain-like polyanionic clusters, like the Te atom to which they are isoelectronic. Similar chain-like polyanions are also found in the alloy of the alkaline-earth elements with tetravalent elements (e.g. Sn^{2-} chains in CrB-type CaSn) [41, 42] and in the Li-rich compounds with Ga and Al (Ga and Al zigzag chains in Li_2Ga and in Li_9Al_4) [43–46].

Like in these polyanionic structures, the picture of Sb^- chains does not imply that the electronic density in the alkali spheres is very small. Indeed an integration of the electron density over the atomic spheres shows that they are almost neutral—the precise results depend rather sensitively on the choice of the radii for the atomic spheres. However, even though the electrons remain close to the alkali sites, they are dominated by the strong attractive Sb potential and contribute to the formation of covalent Sb–Sb bonds.

5. Equiatomic Bi compounds

Unlike the monoantimonides, the equiatomic compounds of Bi with Li and Na assume

the AuCu structure [1]; no equiatomic compounds of Bi with the heavy alkali metals are known to exist. The crystallographic data are given in table 7. In BiLi the axial ratio is $c/a = 0.89$, leading to unlike-atom distances that are 5.3% shorter than the shortest like-atom distances. In BiNa the axial ratio is close to unity ($c/a = 0.98$), leading to almost equal like- and unlike-atom distances. In the limit $c/a \rightarrow 1$ the structure is cubic close packed. Each atom has four like and eight unlike neighbours.

Table 7. Crystallographic description of AuCu-type Bi compounds.

Pearson symbol tP4, space group $P4/mmm$						
Atomic positions						
Au(1)	(1a)	0	0	0		
Au(2)	(1c)	0.5	0.5	0		
Cu	(2c)	0	0.5	0.5		
Coordination						
	Au	Cu	Total			
Au	4	8	12			
Cu	8	4	12			
Lattice constants, interatomic distances, Wigner–Seitz radii						
AB	a (Å)	c (Å)	d_{AA} (Å)	d_{AB} (Å)	d_{BB} (Å)	R_B/R_A
BiLi	4.762	4.256	3.37	3.19	3.37	0.88
BiNa	4.910	4.810	3.47	3.43	3.47	1.0
Excess volume						
BiLi	−13.8%					
BiNa	−19.8%					

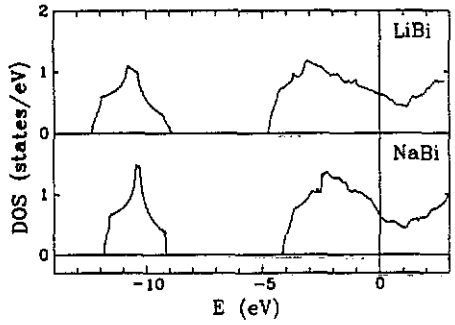

Figure 17. Total electronic density of states in LiBi and NaBi with the AuCu structure.

The total electronic DOS of LiBi and NaBi in the AuCu structure is given in figure 17; the site- and angular-momentum-decomposed DOS for NaBi is shown in figure 18 (the result for LiBi is very similar). We find that the electronic structure is entirely dominated by the strong attractive Bi potential and is similar to that of pure Bi. A low-lying Bi s band is separated by a gap of nearly 5 eV from a Bi p valence band

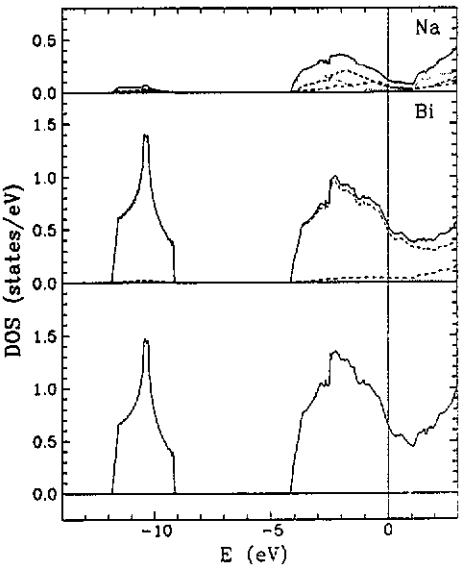

Figure 18. Site- and angular-momentum-decomposed electronic density of states in NaBi. Key: see figure 5.

at the Fermi level. The alkali contribution to the occupied part of the band has an entirely mixed angular momentum character, and originates from the overlap of the Bi p states into the alkali spheres. The onset of the alkali bands is located about 1 eV above the Fermi level; there is a slight overlap with the uppermost part of the Bi p band. The Bi–Bi bond is essentially metallic, like in elemental Bi. There is no indication for a bonding–antibonding splitting in the Bi p band. The Bi–Na bond is partially ionic, but formal ion charges obtained by integrating over atomic spheres are again small.

6. Alkali–bismuth Laves phases

The formation of the A_2B Laves phases is usually considered to be governed by space-filling arguments [38]; ideal space filling is achieved for a radius ratio of $R_B/R_A = 1.225$. For KBi_2, the ratio of the atomic radii, $R_K/R_{Bi} = 1.27$ is rather close to this ideal value so that the formation of a Laves phase is not entirely unexpected. The Laves phases with Rb and Bi can be formed only under a considerable contraction of the alkali–alkali distances ($R_{Cs}/R_{Bi} = 1.47$), and this is possible because of the large compressibilities of the heavy alkali metals. Note that similar compressions occur even in the hexagonal Laves phase $NaCs_2$ [47]. In the alkali–bismuth Laves phases, the Bi–Bi distances are slightly increased (2–5%) relative to elemental Bi (see table 8), whereas the alkali–alkali distances are contracted by 9 to 20%. The total electronic DOS for the three Laves phases is shown in figure 19. We find again a low-lying s band. The structure of this band is determined by the topology of the tetrahedral network of the majority atoms in the Laves phases. A similar result has also been found in the hexagonal KPb_2 Laves phase [25]. The three parts of the band are derived from the molecular orbitals corresponding to the A_1 and T_2 irreducible representations of the Bi tetrahedra. The extremely narrow band originates from the

A_1 level; the three T_2 levels are broadened into a symmetric band. The states close to the Fermi level are Bi p states (the local and partial DOS for $RbBi_2$ is given in figure 20). A pseudogap about 0.8 eV below the Fermi level separates states that are bonding within the tetrahedra from antibonding linear combinations of Bi p states. The bonding states derive from the A_1, T_2 and E irreducible representations, the antibonding bands from the T_1 and T_2 representations. However, due to the large overlap of the p orbitals, the structure within the bonding and antibonding bands is largely smeared out. Another, somewhat shallower pseudogap between 2.2 eV and 2.7 eV above the Fermi level marks the onset of the lowest empty alkali states. In the series (K, Rb, Cs)–Bi_2 these states show increasing d character.

Table 8. Crystallographic description of alkali–Bi Laves phases ($MgCu_2$ type).

Pearson symbol cF24, space group $Fd\bar{3}m$						
Atomic positions						
Mg (8a)	0	0	0			
Cu (16d)	0.625	0.625	0.625			
Coordination						
	Mg	Cu	Total			
Mg	4	12	16			
Cu	6	6	12			
Lattice constants, interatomic distances, Wigner–Seitz radii, excess volume						
A_2B	a (Å)	d_{AA} (Å)	d_{AB} (Å)	d_{BB} (Å)	R_B/R_A	$\Delta\Omega$ (%)
Bi_2K	9.501	3.36	3.94	4.11	1.22	−23.7 %
Bi_2Rb	9.609	3.40	3.98	4.16	1.22	−28.9 %
Bi_2Cs	9.760	3.45	4.04	4.22	1.22	−35.3 %

Thus the electronic DOS of the alkali–bismuth Laves phases is very similar to that of the alkali–lead Laves phases and is related to the electronic structure of the alkali–lead (tin) cluster compounds. In the equiatomic alkali–lead (tin) compounds, tetrahedral Pb_4^{4-} clusters are stabilized by covalent three-centre bonds as in P_4 molecules [4]. This bond is very strong and is also found in the molten alloys and in the KPb_2 Laves phase. Here we find that the same type of bonding is also found in the Bi compound. The only difference is that in the alkali–lead phases the Fermi level falls just below the pseudogap, while in the alkali–bismuth phases it is just above. This demonstrates that the bonding mechanism is not very sensitive to the precise degree of band filling.

7. Discussion

We have found that the electronic structure of all alkali–pnictide compounds, ranging from the ionic octet compounds to the covalent–ionic chain compounds and to the metallic Bi-rich compounds, is entirely dominated by the strong attractive potential of the pnictide atom. The role of the alkali–metal atoms is to keep the polyvalent atoms apart and to provide a 'bridging' function between the Bi (Sb) atoms or chains.

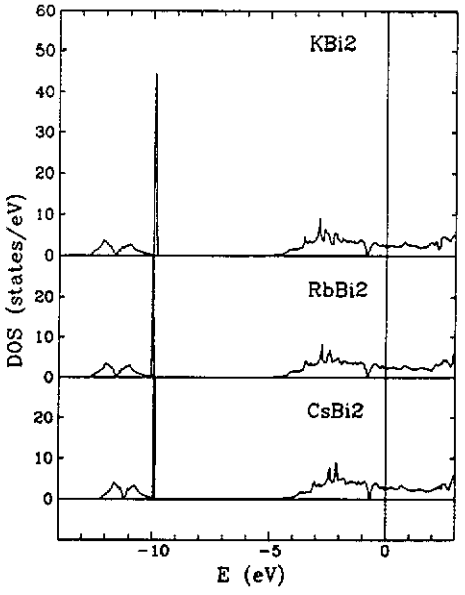

Figure 19. Total electronic density of states in the cubic Laves-phase compounds KBi_2, $RbBi_2$, and $CsBi_2$.

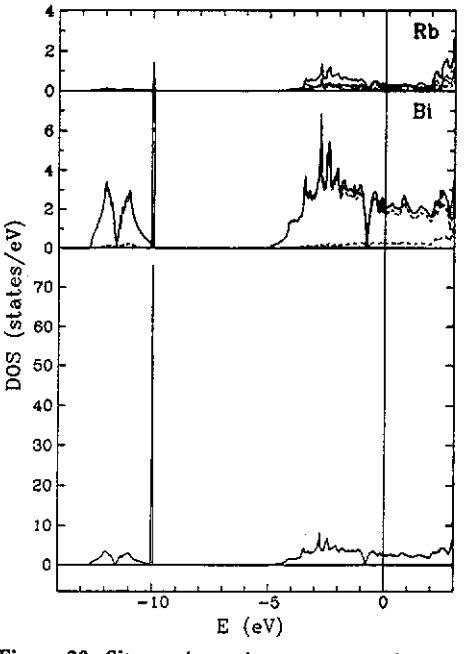

Figure 20. Site- and angular-momentum-decomposed electronic density of states in the Laves-phase compound $RbBi_2$. Key: see figure 5.

In the octet compounds there are no direct Bi (Sb) neighbours. Thus we find narrow bands derived from the energy eigenvalues of the free Bi (Sb) atom. The large

difference in valence leads to a very large negative excess volume, which is rather well described even by low-order perturbation theory. The large volume compression leads to alkali–alkali nearest-neighbour distances that are considerably smaller than in the pure metal. The large electronic pressure on the alkali sites leads to a lowering of the $(n-1)$d states relative to the ns states, especially for the heavy alkalis. The large overlap between the remaining s states at the lower edge of the conduction band causes the formation of bands with a large dispersion and of a low-energy tail of the conduction band. As a consequence, the ionic gap is very narrow and varies in a non-monotonic way in the series (Li, Na, K, Rb, Cs)$_3$–(Sb, Bi). Also it has to be emphasized that due to the overlap of the Bi (Sb) states into the alkali spheres, ionicities defined in terms of net ionic charges are small, so the bonding cannot be termed truly ionic. The comparison of the results obtained for the $BiLi_3$ and $NaAs_3$ structures shows that the lowest conduction band states are very sensitive to the details of the alkali–alkali coordination. Even small displacements of the alkali atoms could lead to a complete disappearance of the gap.

At higher Bi (Sb) concentrations, the overlap between the pnictide states becomes strong enough to stabilize anionic clusters or extended anionic sublattices. According to generalized valence rules, the stable anionic clusters for Sb^- ions are infinitely extended Sb^- chains, similar to those that exist in the isoelectronic elements Se and Te. The electronic structure of the Sb chain compounds is very similar to that of trigonal Se: the valence bands consist of a low-lying Sb s band whose form is characteristic for (ssσ) bonds in chains, and an Sb p band split into bonding, non-bonding and antibonding parts. The Fermi level falls into a covalent gap between the non-bonding and antibonding states. The role of the alkali atoms is to keep the Sb atoms apart and to provide some weak bridging bonds, mainly a coupling between the non-bonding Sb p orbitals oriented parallel to the axis of the chain and the alkali states. However, the fact that the electronic structure of NaSb shows only little difference from that of CsSb shows that this coupling is only very weak. It also suggests that the Sb–Sb bonds will not be very much affected by small displacements of the alkali atoms. Our results for the chain compounds are a nice illustration of the validity of the general Zintl principle.

The main difference between the equiatomic alkali–Sb and alkali–Bi compounds arises from the more extended nature of the Bi 5p orbitals compared to the Sb 4p orbitals. This leads to a strong interchain coupling which destabilizes the chain structures relative to the AuCu structure for the equiatomic alkali–Bi compounds. The electronic structures of the AuCu-type LiBi and NaBi compounds are similar to that of simple-cubic Bi and differ from that of trigonal Bi by the absence of the narrow pseudogaps in the middle of both the s and p bands induced by the Peierls distortion. Thus the AuCu-type compounds are metallic.

At even higher Bi (Sb) content, topologically close-packed phases are formed. The tetrahedral network of Bi atoms in the alkali–Bi Laves phases is stabilized by Bi p three-centre bonds of a relatively pronounced covalent character. However, due to the excess electrons provided by the alkali atoms, the compounds are metallic. The same type of bond is also found in alkali–lead cluster compounds and Laves phases.

In all these compounds, the lowest cation state lies above the highest occupied anion state—hence there is always some charge transfer, although, due to the extended nature of the anion orbitals, formal ionicities defined in terms of net ionic charges are small. If, following Robertson [2], we define a charge-transfer compound this way, this provides a unifying concept for all alkali–pnictide compounds.

Our results allow a tentative interpretation of the surprising results found in the electrical transport properties of the molten alloys: the gap in the octet compounds has been found to be very sensitive to the alkali–alkali correlations. Hence small displacements of the alkali atoms can lead to the formation of a large number of gap states, and to a metallic behaviour of the molten alloy. On the other hand, the electronic structure of the chain compounds is largely independent of the alkali states, due to the more localized nature of the covalent Sb^-–Sb^- bond. Hence the gap can exist even in a disordered medium. However, experience from electronic structure calculations on liquid As [47, 48] and liquid Se [49] shows that this requires well-defined correlations in the chains and relatively strong multi-ion forces. It must be left to future work to confirm these suggestions.

Acknowledgments

This work has been supported by a grant from the Bundesministerium für Wissenschaft und Forschung, Wien. MT acknowledges the support of the Hungarian Science Foundation (OTKA) under grant No 2950.

References

[1] Villars P and Calvert N E 1985 *Pearson's Handbook of Crystallographic Data for Intermetallic Phases* (Metals Park, OH: American Society for Metals)
[2] Robertson J 1983 *Phys. Rev.* B **27** 6322
[3] Moffat W G 1981 *The Handbook of Binary Phase Diagrams* (Schenectady, NY: Genium Publishing)
[4] De Munari G M, Ginsiano F and Mambriani G 1968 *Phys. Status Solidi* b **29** 341
[5] Cromer D T 1959 *Acta Crystallogr.* **12** 36, 41
[6] Busmann E and Lohmeyer S 1961 *Z. Anorg. Allg. Chem.* **312** 53
[7] von Schnering H G, Hönle W and Krogull G 1979 *Z. Naturf.* b **34** 1678
[8] Busmann E and Lohmeyer S 1961 *Z. Anorg. Allg. Chem.* **312** 53
[9] van der Lugt W and Geertsma W 1987 *Can. J. Phys.* **65** 327
[10] Freyland W and Steinleitner G 1977 *Liquids Metals '77 (Inst. Phys. Conf. Ser. 30)* ed R Evans and D A Greenwood (Bristol: Institute of Physics) p 488
[11] Redslob H, Steinleitner G and Freyland W 1982 *Z. Naturf.* a **2** 587
[12] Saboungi M L, Ellefson J, Johnson G K and Freyland W 1988 *J. Chem. Phys.* **88** 5812
[13] Lamparter P, Martin W and Steeb S 1983 *Z. Naturf.* a **38** 329
[14] Lamparter P, Martin W, Steeb S and Freyland W 1984 *J. Non-Cryst. Solids* **61+62** 279
[15] Zintl E, Goubeau J and Dullenkopf W 1931 *Z. Phys. Chem.* A **154** 1
[16] Busmann E 1961 *Z. Anorg. Chem.* **313** 90
[17] Steinleitner G, Freyland W and Hensel F 1975 *Ber. Bunsenges. Phys. Chem.* **79** 1186
[18] Xu R, Kinderman R and van der Lugt W 1991 *J. Phys.: Condens. Matter* **3** 127
[19] Yih T S and Thompson J C 1982 *J. Phys. F: Met. Phys.* **12** 1652
[20] Meijer J A and van der Lugt W 1989 *J. Phys. C: Solid State Phys.* **1** 9779
[21] Petric J A, Pelton A D and Saboungi M L 1989 *J. Phys. F: Met. Phys.* **18** 1473
[22] Petric A, Pelton A D and Saboungi M L 1988 *J. Electrochem. Soc.* **135** 2744
[23] Springelkamp F, de Groot R A, Geertsma W, van der Lugt W and Mueller F M 1985 *Phys. Rev.* B **32** 2319
[24] Geertsma W 1985 *J. Phys. C: Solid State Phys.* **18** 2416
[25] Tegze M and Hafner J 1989 *Phys. Rev.* B **39** 8263
[26] Tegze M and Hafner J 1989 *Phys. Rev.* B **40** 9841
[27] Robertson J 1992 *Solid State Commun.* **47** 899
[28] Robertson J 1983 *Adv.Phys.* **32** 361
[29] Christensen N E 1984 *Phys. Rev.* B **30** 5733

[30] Andersen O K, Jepsen O and Glötzel D 1985 *Highlights of Condensed Matter Theory* ed F Bassani, F Fumi and M P Tosi (Amsterdam: North-Holland)
[31] Skriver H 1981 *The LMTO Method* (Berlin: Springer)
[32] Cohen M H and Chelikowsky J R 1988 *Electronic Structure and Optical Properties of Semiconductors* (Berlin: Springer)
[33] Littlewood P B 1983 *Crit. Rev. Solid State Mater. Sci.* **11** 229; 1983 *J. Phys. C: Solid State Phys.* **13** 4855, 4875
[34] von Barth U, Hedin L and Janak J F 1975 *Phys. Rev.* B **12** 1257
[35] Jepsen O and Andersen O K 1971 *Solid State Commun.* **9** 1763
[36] Lehmann G and Taut M 1972 *Phys. Status Solidi* b **54** 469
[37] Hafner J 1985 *J. Phys. F: Met. Phys.* **15** L43
[38] Pearson W B 1972 *The Crystal Chemistry and Physics of Metals and Alloys* (New York: Wiley)
[39] Katayama Y, Yao M, Ajiro Y, Inu M and Endo H 1989 *J. Phys. Soc. Japan* **58** 1811
[40] Ikawa A and Fukutome H 1990 *J. Phys. Soc. Japan* **59** 1002, 4041
[41] Parthé E 1981 *Structure and Bonding in Crystals* vol II, ed M O'Keefe and A Navrotsky (New York: Academic) p 259
[42] Tegze M and Hafner J 1989 *J. Phys.: Condens. Matter* **1** 8293
[43] Müller W and Stöhr J 1977 *Z. Naturf.* b **32** 631
[44] Hafner J, Jank W and Holzmannhofer J 1992 *J. Non-Cryst. Solids* at press
[45] Guo X Q, Podloucky R and Freeman A J 1990 *Phys. Rev.* B **42** 10912
[46] Hafner J and Jank W 1991 *Phys. Rev.* B **44** 11662
[47] Hafner J 1977 *Phys. Rev.* B **15** 671